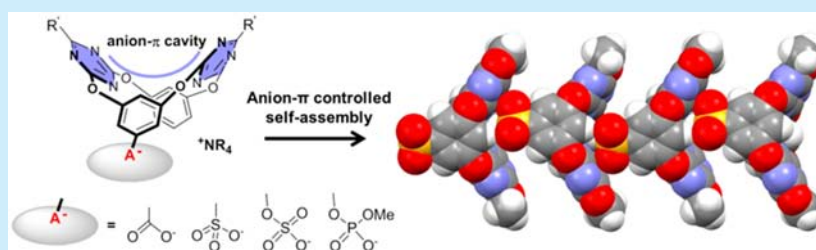


Anionic Head Containing Oxacalix[2]arene[2]triazines: Synthesis and Anion- π -Directed Self-Assembly in Solution and Solid StateRui-Bin Xu,^{†,‡} Qi-Qiang Wang,^{*,†,‡,§} Yu-Fei Ao,[†] Zhi-Yan Li,[†] Zhi-Tang Huang,[†] and De-Xian Wang^{*,†,‡,§}[†]Beijing National Laboratory for Molecular Sciences, CAS Key Laboratory of Molecular Recognition and Function, Institute of Chemistry, Chinese Academy of Sciences, Beijing 100190, China[‡]University of Chinese Academy of Sciences, Beijing 100049, China

§ Supporting Information



ABSTRACT: A series of oxacalix[2]arene[2]triazines bearing one anionic head such as carboxylate, sulfonate, sulfate, and phosphate were synthesized. With the anionic head and complementary V-shape electron-deficient cavity, these macrocycles can serve as dual building units, and their anion- π directed self-assembly was investigated. The formation of oligomeric aggregates in solution was revealed by nuclear magnetic resonance, dynamic light scattering, and mass spectroscopy. Crystal structures further confirmed chainlike assembly formation directed by anion- π interactions.

Self-assembly is a central theme in supramolecular chemistry. Compared to numerous studies where the cation directs assembly formation, e.g., metal-coordination-driven self-assembly, roles of anion on self-assembly have been neglected and only realized recently.¹ This is not surprising as incorporation of anions into an assembly entity is a challenging task due to their large size, varied geometry, high solvation free energy, and less directional interaction.² Generally, anions can participate in self-assembly through interactions including electrostatic attraction,³ metal coordination (Lewis acid-base interaction),⁴ hydrogen bonding,⁵ and halogen bonding.⁶ Recently, a novel noncovalent interaction between anion and electron-deficient arene, namely, anion- π interaction, has received great interest.⁷ Although a number of cation-controlled assembly systems with concurrency of anion- π interaction have been reported,⁸ in these systems, anion- π interaction is usually auxiliary and barely affects the assembly entity. Examples of anion-directed self-assembly where anion- π interaction plays a decisive role remain rare.^{7e,9,10} In the few reported studies, anion mainly serves as a template inducing specific aggregation in the course of transition-metal-based assembly formation. For example, Dunbar and co-workers examined the role of anion- π interactions on templating the formation of different numbered cyclic metal-assembled architectures depending on the specific counteranion used.⁹ However, with metal ion, it is difficult to distinguish the contribution between anion- π interaction and intrinsic Coulombic interaction. Therefore, using charge-neutral π receptor as a building component to probe anion- π -directed assembly is particularly

intriguing. In this regard, our group reported the formation of various supramolecular structures driven by typical anion- π interactions, including cage,^{10a} honeycomb,^{10b} and linear wire.^{10c} Meanwhile, 1D linear wire formation driven by σ -type and the combination of σ -type and typical anion- π interactions was demonstrated by the groups of Kochi¹¹ and Dunbar,¹² respectively. Very recently, we realized anion- π interaction is able to direct the supramolecular amphiphile formation between oxacalix[2]arene[2]triazine and anionic amphiphile, which is crucial for the subsequent assembly to form vesicle.¹³ It should also be noted that anion- π controlled self-assembly is currently investigated mainly in the solid state, as systematic study in solution is challenging. On the basis of our previous studies, the persistent V-shape cavity of oxacalix[2]arene[2]triazine can accommodate anion through anion- π interactions. We envisioned that incorporating an anionic head (e.g., carboxylate, sulfonate, sulfate, and phosphate) onto the host skeleton could render the macrocycle as a self-complementary building unit for anion- π directed self-assembly (Figure 1). Reported herein are the synthesis and systematical investigation of self-assembly behavior in both solution and the solid state.

As depicted in Scheme 1, 3 + 1 fragment coupling between trimer 1 and functionalized monomers 2 followed by debenzoylation (in case of 2a and 2c) gave the corresponding oxacalix[2]arene[2]triazine derivatives 3a-c in moderate yields.

Received: January 9, 2017

Published: January 19, 2017

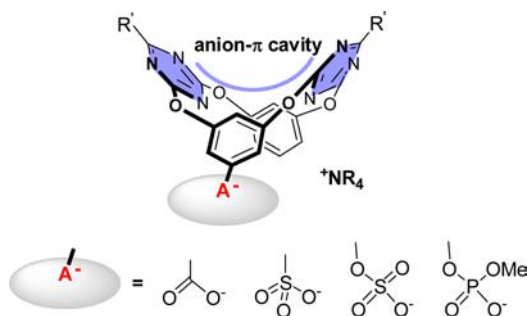
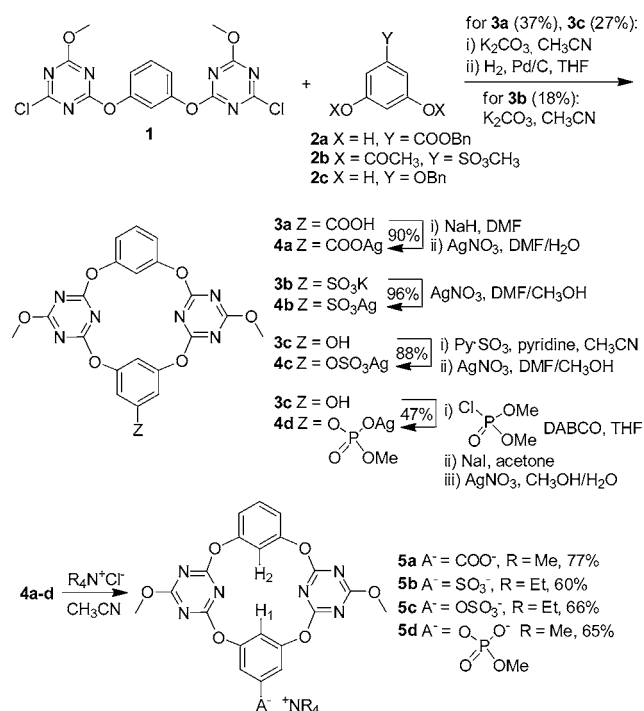


Figure 1. Incorporating an anionic head onto oxalix[2]arene[2]triazine for anion- π directed assembly.

Scheme 1. Synthesis of Assembly Building Blocks 5a–d



Converting **3a** to sodium salt with NaH and then treatment with AgNO_3 led to silver salt **4a** in 90% yield. Treating **3b** with AgNO_3 directly gave silver salt **4b** in 96% yield. To synthesize **4c** and **4d**, **3c** was first reacted with pyridine sulfur trioxide and dimethyl chlorophosphate, respectively, followed by demethylation in case of **4d**, and further treatment with AgNO_3 furnished the silver salts in good yields. All the silver salts can be readily converted to tetramethylammonium or tetraethylammonium salts **5a–d** in 60–77% yields.

As electronic density of triazine ring is vital for anion- π interaction,¹⁴ the electron deficiency of the V-shape cavity in **5** was first probed by using dimethoxy-substituted oxalix[2]arene[2]triazine (without the anionic head) as a model host (Supporting Information). Different anion guests, including acetate, methanesulfonate, methyl sulfate, and methyl phenyl phosphate (as tetraalkylammonium salts) were used to mimic the anionic head in **5**. Upon titration of methanesulfonate, methyl sulfate, and methyl phenyl phosphate, fluorescent emission intensity of the model host in the range of 350–400 nm gradually increased, and for acetate a new emission band at 450 nm emerged. The Job's plot indicated 1:1 complex formation, and the calculated association constants (K_a) are in the

range of 1131–9598 M^{-1} (Figures S1–S4). These results imply that in **5a–d** the V-shape cavity could form anion- π interaction with the anionic head of another macrocycle molecule (there is no way for intramolecular interaction due to the rigid conformation). Similar to model host-acetate complexation, for **5a**, an emission peak at 450 nm was observed as well (disappeared at a low concentration), suggesting similar donor-acceptor interaction (Figure S5). Moreover, for **5a–d**, in all cases the fluorescent intensity at maximum emission wavelength showed non-linear concentration-dependent increase from 1.3×10^{-5} to 1.0×10^{-3} M. This nonlinear trend is significantly larger than that of the model host (Figure S9). This indicated that self-aggregation of **5a–d** upon increasing concentration may contribute to the large nonlinear effect.

According to a recent theoretical study,¹⁵ in addition to the ubiquitous anion- π interaction between anion and triazine rings of oxalix[2]arene[2]triazine, the low-rim hydrogen atom (e.g., H₁, H₂, toward the cavity) can concurrently participate the anion binding via weak hydrogen bonding in the existence of triangle and octahedral anion. This prediction implies that the self-assembly behavior of **5a–d** could be probed by NMR through monitoring the chemical shift changes of related proton signals. Hence, ¹H NMR spectra of **5a–d** at variable concentrations were recorded. As shown in Figure 2 and Figures S10–S14, H₁ and H₂ did downfield shift gradually upon increasing concentration, while other proton signals almost remained intact. This suggests that intermolecular interaction would occur with the anionic

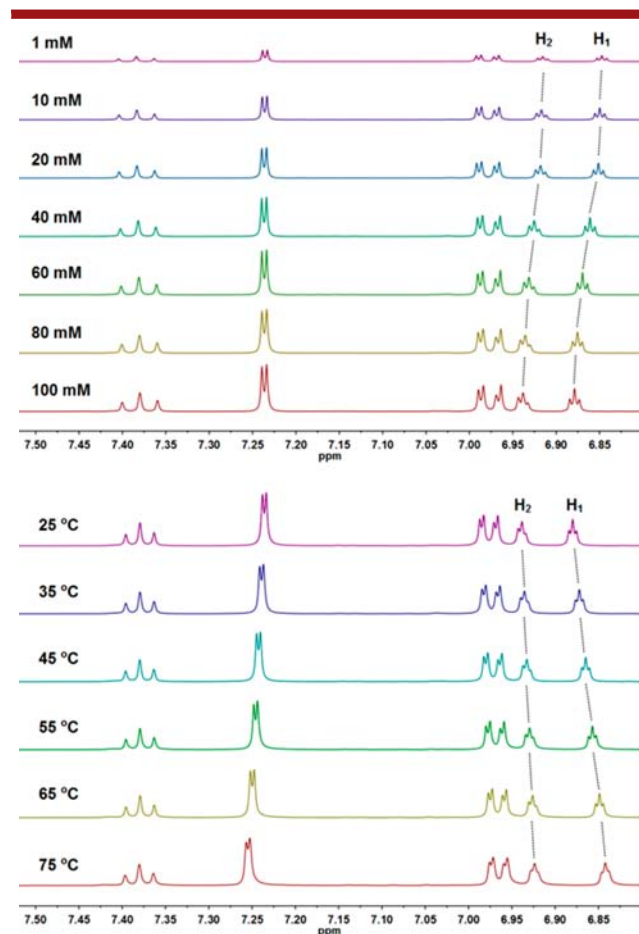


Figure 2. ¹H NMR spectra of **5b** in CD_3CN . Top, variable concentrations (298 K). Bottom, variable temperatures (100 mM).

head being included within the V-shape cavity of another molecule. H₁ and H₂ therefore concurrently participate in the anion binding through weak hydrogen bonding¹⁵ along with the dominant anion- π interaction. The assembly behavior was further confirmed by variable-temperature (VT) ¹H NMR where an upfield shift of H₁ and H₂ was observed from 25 to 75 °C, in line with disfavored assembly (disassembly) at elevated temperature (Figure 2 and Figures S10–S14).

The supramolecular aggregation was further investigated by diffusion-ordered NMR spectroscopy (DOSY). In order to avoid inaccuracy brought by the viscosity change at variable concentrations, the residual solvent peak (dichloromethane) was used as an internal reference. As the hydrodynamic radius of dichloromethane is considered constant upon concentration change, variation on the ratio of diffusion coefficients, $D(\text{compound})/D(\text{CH}_2\text{Cl}_2)$, would reflect the hydrodynamic radius change for the aggregates existed in solution. As expected, in all cases for **5a–d**, the ratio of $D(\text{compound})/D(\text{CH}_2\text{Cl}_2)$ gradually decreased upon increasing concentration (Tables S1–S4), indicating larger and larger assembly formation during the course. The aggregation behavior was also evidenced by dynamic light scattering (DLS). In all four cases **5a–d**, a single scattering band was observed and the corresponding hydrodynamic radius gradually increased upon increasing sample concentration (for example of **5b**: 0.86, 1.38, 1.76, and 2.24 nm at 5, 10, 20, and 30 mM, respectively, Tables S5–S8 and Figures S19–S22).

The aggregation was further evidenced by electrospray ionization mass spectrometry (ESI-MS). As shown in Figure 3 and

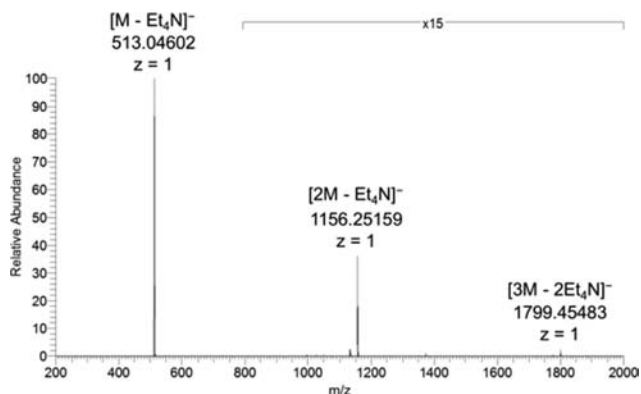


Figure 3. ESI-MS (negative mode) spectrum of **5b**.

Figures S31–S34, except for monomeric peak $[M - \text{Et}_4\text{N}]^-$, a series of dimeric $[2M - \text{Et}_4\text{N}]^-$ and trimeric $[3M - 2\text{Et}_4\text{N}]^-$ peaks were also observed. The higher oligomeric peaks could not be observed, probably due to detection limitations and the instability of larger assembly species on ionization conditions.

Single-crystal structures gave more insight into the assembly details in the solid state. As expected, for all three compounds **5a–c**, the anionic head is included within the V-shape cavity of another adjacent molecule through anion- π interactions along with weak hydrogen bonding (Figures 4–6). As such, 1D linear assembly was formed. For **5a**, the benzoate moiety is accommodated by the V-shape cavity. One carboxylate oxygen atom (O6) locates over one triazine with an O-plane distance ($d_{\text{O6-plane}}$) of 3.283 Å, forming a typical noncovalent anion- π interaction. The other oxygen atom (O5) interacts peripherally with the other triazine through σ -type interaction ($d_{\text{O5-C8}} = 3.353$ Å). Meanwhile, one inward hydrogen (H6) is involved in the anion binding through weak hydrogen bonding ($d_{\text{O5-C6}} = 3.302$ Å). For the

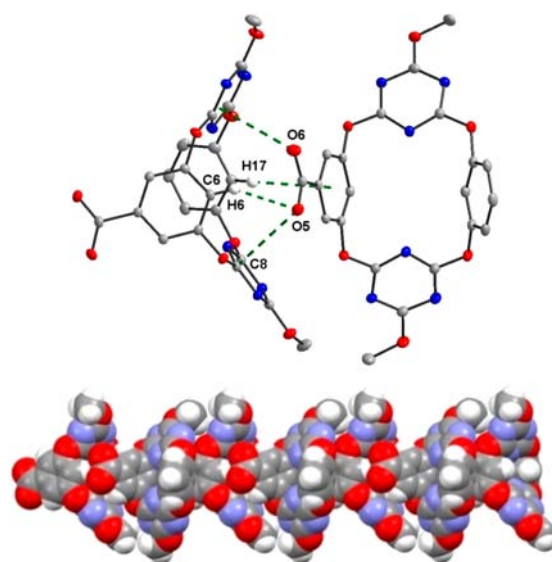


Figure 4. Crystal structure of **5a**. (Top) Dimeric motif showing benzoate moiety lying within the V-shape cavity of adjacent molecule through cooperative anion- π , H-bonding, and C-H- π interactions. (Bottom) 1D chainlike assembly motif. Counteranion $^+\text{NMe}_4$ and solvent CH_3CN molecules are omitted for clarity.

other hydrogen (H17), judged from the short contact with the benzoate plane ($d_{\text{H17-plane}} = 2.909$ Å), weak C-H- π interaction may exist. With the orthogonal alignment of the two staggered macrocyclic skeletons, the dimeric binding motif extends to form an infinite zigzag assembly (Figure 4).

Different from **5a**, for **5b** only the sulfonate head inserts within the cavity, and the linked benzene moiety stays upright and apart from the V-shape cavity (Figure 5). Owing to the tetrahedral geometry of sulfonate, for the three triangle oxygen atoms, O7 locates almost above the center of the triazine with a short anion- π interaction distance ($d_{\text{O7-plane}} = 2.906$ Å); the other two oxygens O5 and O6 concurrently interact with the two inward hydrogen atoms through hydrogen bonding. Unlike the orthogonal alignment in **5a**, the adjacent macrocyclic skeletons in **5b**

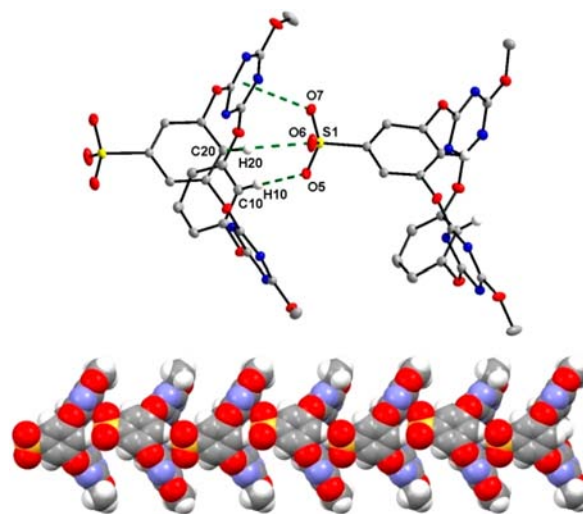


Figure 5. Crystal structure of **5b**. (Top) Dimeric motif showing sulfonate head inserting into the V-shape cavity of the adjacent molecule through anion- π and H-bonding interactions. (Bottom) 1D chainlike assembly motif. Counteranion $^+\text{NEt}_4$ is omitted for clarity.

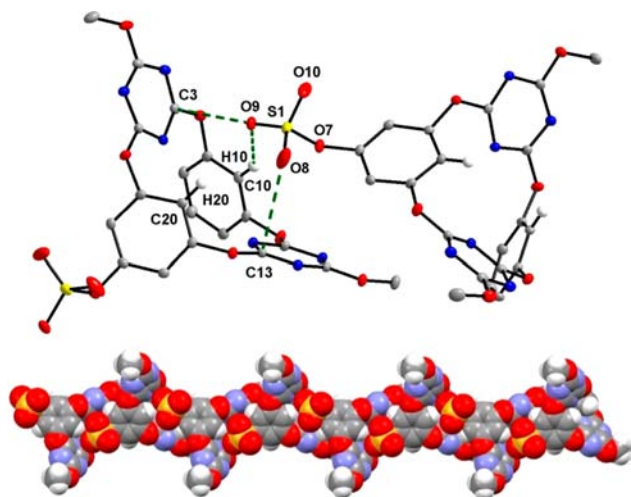


Figure 6. Crystal structure of **5c**. (Top) Dimeric motif showing sulfate head inserting into V-shape cavity of adjacent molecule through anion- π and H-bonding interactions. (Bottom) 1D chainlike assembly motif. Counteranion $^+NEt_4$ is omitted for clarity.

align in parallel and extend to form a nicely linear assembly. For **5c**, the sulfate head forms σ -type anion- π interactions with the two triazine rings simultaneously, accompanied by weak hydrogen bonding with one inward hydrogen (Figure 6). The macrocyclic skeletons are more staggered in the extended assembly motif probably due to the offset of the sulfate head from the attached benzene ring plane.

In summary, a series of oxalix[2]arene[2]triazine derivatives **5a–d** incorporating one anionic head on the benzene ring upper rim were efficiently synthesized. The macrocyclic unit can act as a dual self-complementary building block to form oligomeric aggregate in both solution and solid state. Anion- π interaction between the anionic head and the V-shape electron-deficient cavity plays a decisive role to direct the assembly formation. This strategy hence demonstrates that tailor-made oxalix[2]arene[2]triazine can be a promising building component to address the challenging anion- π directed self-assembly. Applying such a system in order to obtain a discrete assembly architecture (e.g., cyclic) and taking charge-neutral oxalix[2]arene[2]triazine with discrete anion to achieve controlled self-assembly are currently underway in this laboratory.

■ ASSOCIATED CONTENT

Supporting Information

The Supporting Information is available free of charge on the ACS Publications website at DOI: [10.1021/acs.orglett.7b00070](https://doi.org/10.1021/acs.orglett.7b00070).

Synthesis procedure, characterization, fluorescent spectra, and additional NMR, DLS, and ESI-MS spectra (PDF)

Crystallographic data of **5a** (CIF)

Crystallographic data of **5b** (CIF)

Crystallographic data of **5c** (CIF)

■ AUTHOR INFORMATION

Corresponding Authors

*Email: qiqiangw@iccas.ac.cn

*Email: dxwang@iccas.ac.cn

ORCID 

Qi-Qiang Wang: 0000-0001-5988-1293

De-Xian Wang: 0000-0002-9059-5022

Notes

The authors declare no competing financial interest.

■ ACKNOWLEDGMENTS

Financial support from NSFC (21272239, 91427301, 21502200, 21521002) and MOST (2013CB834504) is gratefully acknowledged. Q.-Q.W. also thanks the Thousand Young Talents Program for support.

■ REFERENCES

- (1) Custelcean, R. *Chem. Soc. Rev.* **2010**, 39, 3675–3685.
- (2) Bowman-James, K.; Bianchi, A.; Carcia-España, E. *Anion Coordination Chemistry*; Wiley-VCH, 2012.
- (3) Sánchez-Quesada, J.; Seel, C.; Prados, P.; de Mendoza, J.; Dalcol, I.; Giralt, E. *J. Am. Chem. Soc.* **1996**, 118, 277–278.
- (4) Noro, S.-i.; Kitaura, R.; Kondo, M.; Kitagawa, S.; Ishii, T.; Matsuzaka, H.; Yamashita, M. *J. Am. Chem. Soc.* **2002**, 124, 2568–2583.
- (5) (a) Wu, B.; Cui, F.; Lei, Y.; Li, S.; de Sousa Amadeu, N.; Janiak, C.; Lin, Y.-J.; Weng, L.-H.; Wang, Y.-Y.; Yang, X.-J. *Angew. Chem., Int. Ed.* **2013**, 52, 5096–5100. (b) Byrne, P.; Lloyd, G. O.; Anderson, K. M.; Clarke, N.; Steed, J. W. *Chem. Commun.* **2008**, 3720–3722. (c) Wang, Y.; Xiang, J.; Jiang, H. *Chem. - Eur. J.* **2011**, 17, 613–619.
- (6) (a) Metrangolo, P.; Pilati, T.; Terraneo, G.; Biella, S.; Resnati, G. *CrystEngComm* **2009**, 11, 1187–1196. (b) Evans, N. H.; Beer, P. D. *Angew. Chem., Int. Ed.* **2014**, 53, 11716–11754.
- (7) (a) Gamez, P.; Mooibroek, T. J.; Teat, S. J.; Reedijk, J. *Acc. Chem. Res.* **2007**, 40, 435–444. (b) Hay, B. P.; Bryantsev, V. S. *Chem. Commun.* **2008**, 2417–2428. (c) Frontera, A.; Gamez, P.; Mascal, M.; Mooibroek, T. J.; Reedijk, J. *Angew. Chem., Int. Ed.* **2011**, 50, 9564–9583. (d) Wang, D.-X.; Wang, M.-X. *Chimia* **2011**, 65, 939–943. (e) Chifotides, H. T.; Dunbar, K. R. *Acc. Chem. Res.* **2013**, 46, 894–906. (f) Watt, M.; Collins, M. S.; Johnson, D. W. *Acc. Chem. Res.* **2013**, 46, 955–966. (g) Ballester, P. *Acc. Chem. Res.* **2013**, 46, 874–884. (h) Vargas Jentzsch, A.; Hennig, A.; Mareda, J.; Matile, S. *Acc. Chem. Res.* **2013**, 46, 2791–2800. (i) Gamez, P. *Inorg. Chem. Front.* **2014**, 1, 35–43. (j) Giese, M.; Albrecht, M.; Rissanen, K. *Chem. Commun.* **2016**, 52, 1778–1795.
- (8) (a) de Hoog, P.; Gamez, P.; Mutikainen, I.; Turpeinen, U.; Reedijk, J. *Angew. Chem., Int. Ed.* **2004**, 43, 5815–5817. (b) Demeshko, S.; Dechert, S.; Meyer, F. *J. Am. Chem. Soc.* **2004**, 126, 4508–4509. (c) Brooker, S.; White, N. G.; Bauzá, A.; Deyà, P. M.; Frontera, A. *Inorg. Chem.* **2012**, 51, 10334–10340.
- (9) (a) Campos-Fernández, C. S.; Schottel, B. L.; Chifotides, H. T.; Bera, J. K.; Bacsá, J.; Koomen, J. M.; Russell, D. H.; Dunbar, K. R. *J. Am. Chem. Soc.* **2005**, 127, 12909–12923. (b) Chifotides, H. T.; Giles, I. D.; Dunbar, K. R. *J. Am. Chem. Soc.* **2013**, 135, 3039–3055.
- (10) (a) Wang, D.-X.; Fa, S.-X.; Liu, Y.; Hou, B.-Y.; Wang, M.-X. *Chem. Commun.* **2012**, 48, 11458–11460. (b) Wang, D.-X.; Wang, Q.-Q.; Han, Y.; Wang, Y.; Huang, Z.-T.; Wang, M.-X. *Chem. - Eur. J.* **2010**, 16, 13053–13057. (c) Liu, W.; Wang, Q.-Q.; Wang, Y.; Huang, Z.-T.; Wang, D.-X. *RSC Adv.* **2014**, 4, 9339–9342.
- (11) (a) Rosokha, Y. S.; Lindeman, S. V.; Rosokha, S. V.; Kochi, J. K. *Angew. Chem., Int. Ed.* **2004**, 43, 4650–4652. (b) Han, B.; Lu, J.; Kochi, J. K. *Cryst. Growth Des.* **2008**, 8, 1327–1334.
- (12) Chifotides, H. T.; Schottel, B. L.; Dunbar, K. R. *Angew. Chem., Int. Ed.* **2010**, 49, 7202–7207.
- (13) He, Q.; Ao, Y.-F.; Huang, Z.-T.; Wang, D.-X. *Angew. Chem., Int. Ed.* **2015**, 54, 11785–11790.
- (14) Wang, D.-X.; Zheng, Q.-Y.; Wang, Q.-Q.; Wang, M.-X. *Angew. Chem., Int. Ed.* **2008**, 47, 7485–7488.
- (15) Xi, J.; Xu, X. *Phys. Chem. Chem. Phys.* **2016**, 18, 6913–6924.